analytical chemistry

ARTICLE

pubs.acs.org/ac

# Digital Isothermal Quantification of Nucleic Acids via Simultaneous Chemical Initiation of Recombinase Polymerase Amplification Reactions on SlipChip

Feng Shen,[†] Elena K. Davydova,[†] Wenbin Du,[†] Jason E. Kreutz,[†] Olaf Piepenburg,[‡] and Rustem F. Ismagilov*[,†]

[†]Department of Chemistry and Institute for Biophysical Dynamics, The University of Chicago, 929 East 57th Street, Chicago, Illinois 60637, United States

[‡]TwistDX Limited, Cambridge, United Kingdom

Supporting Information

**ABSTRACT:** In this paper, digital quantitative detection of nucleic acids was achieved at the single-molecule level by chemical initiation of over one thousand sequence-specific, nanoliter isothermal amplification reactions in parallel. Digital polymerase chain reaction (digital PCR), a method used for quantification of nucleic acids, counts the presence or absence of amplification of individual molecules. However, it still requires temperature cycling, which is undesirable under resource-limited conditions. This makes isothermal methods for nucleic acid amplification, such as recombinase polymerase amplification (RPA), more attractive. A microfluidic digital RPA SlipChip is described here for simultaneous initiation of over one thousand nL-scale RPA reactions by adding a chemical initiator to each reaction compartment with a simple slipping step after instrument-free pipet loading. Two designs of the SlipChip, two-step slipping and one-step slipping, were validated using digital RPA. By using the digital RPA SlipChip, false-positive results from preinitiation of the RPA amplification reaction before incubation were eliminated. End point fluorescence readout was used for "yes or no" digital quantification. The performance of digital RPA in a SlipChip was validated by amplifying and counting single molecules of the target nucleic acid, methicillin-resistant *Staphylococcus aureus* (MRSA) genomic DNA. The digital RPA on SlipChip was also tolerant to fluctuations of the incubation temperature (37−42 °C), and its performance was comparable to digital PCR on the same SlipChip design. The digital RPA SlipChip provides a simple method to quantify nucleic acids without requiring thermal cycling or kinetic measurements, with potential applications in diagnostics and environmental monitoring under resource-limited settings. The ability to initiate thousands of chemical reactions in parallel on the nanoliter scale using solvent-resistant glass devices is likely to be useful for a broader range of applications.

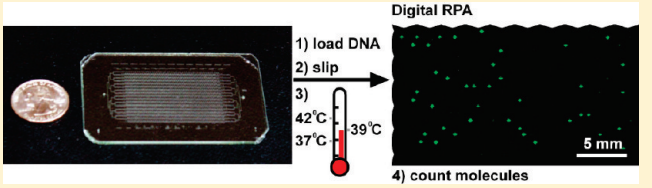


This paper demonstrates a SlipChip for highly parallel chemical initiation of reactions, validated by performing digital isothermal quantification of nucleic acids in a sequence-specific manner by using recombinase polymerase amplification (RPA). Quantitative analysis of nucleic acids is important for studying gene expression[1] and molecular diagnostics, such as for detection of pathogens,[2−4] analysis of genomic diseases and cancer,[5,6] monitoring of viral load,[7−9] and prenatal diagnostics.[10,11] For quantitative nucleic acid analysis methods to be used at the point of care, such as in resource-limited settings or in-home medicine, they must be simple, inexpensive, and easy to use. The most widely used method for nucleic acid amplification and quantitative analysis is real-time polymerase chain reaction (PCR)[12] and real-time reverse-transcription polymerase chain reaction (RT-PCR).[13] Real-time methods are based on the detection of an exponential increase of fluorescence intensity and rapid thermal cycling between the dissociation temperature (∼95 °C), annealing temperature (∼50 °C), and synthesis temperature (∼70 °C).

Digital PCR is another method for quantitative analysis of nucleic acids.[5,14,15] By dividing the diluted sample into a large number of small-volume reaction compartments, single copies of nucleic acid template can be confined in isolated compartments and amplified by PCR. Only a "yes or no" readout is required, and the number of target molecules in the sample is determined by performing a statistical analysis on the number of "positive" and "negative" wells. This method transfers the exponential amplification profile into a linear, digital format. Digital PCR can be performed in a variety of formats, including well plates,[5] microdroplets,[16−18] pneumatic-controlled microchips,[19] spinning discs,[20] OpenArray,[21] and the SlipChip.[22] Although some of these methods have considerably simplified the process of generating a large number of individual, small-volume reaction

**Received:** January 28, 2011
**Accepted:** March 25, 2011
**Published:** April 08, 2011

compartments, an essential step for digital amplification, these digital PCR methods still require thermal cycling and accurate temperature control.

To avoid thermal cycling, different isothermal amplification methods have been developed, such as loop-mediated amplification (LAMP),[23] nucleic acid sequence based amplification (NASBA),[24] recombinase polymerase amplification (RPA),[25] rolling circle amplification (RCA),[26] helicase-dependent amplification (HDA),[27] transcription-mediated amplification (TMA),[28,29] multiple displacement amplification (MDA),[30] and strand-displacement amplification (SDA).[31,32] RCA has been demonstrated in a digital format by using a droplet-based microfluidic platform to amplify a bacterial plasmid,[33] but this method still requires a fluidic pump to accurately control the fluidic flow in order to generate uniform droplets and RCA only works with a circular nucleic acid template. Moreover, the preparation step before incubation was done on ice to avoid preamplification, since RCA is generally performed at 30 °C. Digital MDA was also developed to quantify nucleic acid contamination independent of sequence.[34] However, this method cannot be used to detect and quantify a specific gene sequence, which is desirable for molecular diagnostics. In addition, preamplification is still a potential problem for this digital MDA platform. LAMP has been incorporated on a microchip and a microchamber,[35] but it still requires a heating mechanism to maintain the reaction temperature at 63 °C, which may not be ideal for a point-of-care device in resource-limited settings. NASBA and RPA have also been integrated on a microchip platform with a real-time fluorescence imaging system or an absorbance measurement system for quantitative analysis.[36−38] However, these real-time methods of isothermal amplification are sensitive to temperature because the enzyme activity is highly temperature-dependent. To avoid effects of temperature changes and fluctuations, calibration must be done in parallel to quantitatively analyze nucleic acids. Moreover, most of the methods for detection and analysis of nucleic acids using NASBA and RPA still depend on interpreting exponential amplification profiles.

Although digital PCR requires thermal cycling and accurate temperature control, it is straightforward because initiation of the amplification reaction is controlled by temperature. Special "hot-start" modifications of PCR polymerases are now widely used and essentially eliminate any low-temperature nonspecific preamplification.[39] Therefore, the PCR reaction mixture can be compartmentalized prior to initiation with minimal risk of false-positives due to preinitiation. In situations where the infrastructure for thermal cycling is readily available, digital PCR is an attractive option for nucleic acid quantification. In limited-resource or point-of-care settings, digital isothermal amplification methods that take place at temperatures near room temperature (such as RPA) are advantageous because they do not rely on temperature for initiation but, rather, rely on chemistry. However, if the nucleic acid target is premixed with the initiation reagent prior to compartmentalization, one would expect the amplification reaction to proceed even at room temperature and thus increase the target count. Therefore, to perform digital isothermal nucleic acid amplification, one needs to compartmentalize the sample containing the nucleic acid target prior to adding the initiation reagents. In principle, this multistep manipulation is doable with valves[40,41] and droplets,[33,42−46] but would require complex control systems and instrumentation, so in our opinion, it could be most simply achieved on a SlipChip.

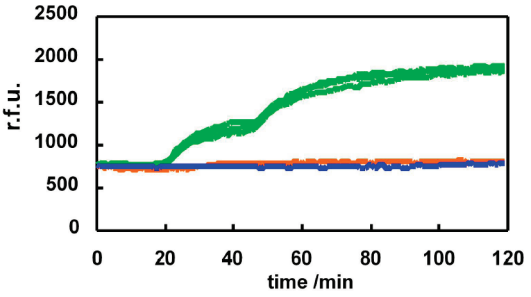


**Figure 1.** RPA amplification of MRSA genomic DNA (5 pg/$\mu$L) in a well plate at 25 °C. Triplicate curves (green lines) show that gDNA template was amplified at room temperature. The control experiment without template (orange line) and the control experiment without magnesium acetate ($Mg(OAc)_2$, blue line) show no amplification.

The SlipChip is a microfluidic platform that enables such multistep manipulation of large numbers of small volumes in parallel.[47,48] The SlipChip has been used to perform protein crystallization,[49,50] immunoassays,[48] multiplex PCR,[51] and digital PCR.[22] The SlipChip consists of two plates containing wells and ducts that can be brought in contact and moved relative to one another to manipulate fluids by creating and breaking fluidic paths. The pattern of wells and ducts in the two plates can contain almost any program to manipulate fluid volumes; compartmentalizing a sample into many small volumes and mixing each small volume with a reagent can be performed by simple subsequent slipping of the two plates.

In this paper, we describe a SlipChip to perform digital isothermal amplification by using RPA. We have demonstrated that digital RPA did not require precise temperature control, as we obtained equivalent quantification results when quantifying methicillin-resistant *Staphylococcus aureus* genomic DNA (MRSA gDNA) at 37, 39, and 42 °C. The technical advance illustrated here is the capability to first confine individual target molecules into separate reaction compartments, and then deliver chemical initiators to initiate all reactions in parallel, a requirement of digital RPA. This SlipChip can also be applied to perform other high-throughput chemical reactions or screenings which require multistep processes such as confinement of one reagent and then addition of subsequent reagents in sequence.

## RESULTS AND DISCUSSION

The mechanism of DNA amplification and fluorescence signal generation facilitated by RPA is described in greater detail elsewhere.[25] Briefly, RPA uses nucleoprotein complexes consisting of oligonucleotide primers and recombinase proteins to target binding sites within template DNA. Upon their binding, the primers are extended by strand-displacing polymerases, thereby copying the target sequence. The use of primers binding to the opposing strands of the template initiates a process of exponential DNA amplification. The generation of amplified target material can be monitored by an appropriate oligonucleotide-probe-based fluorescence detection system. In the approach used here, a fluorophore/quencher bearing probe is nucleolytically cut in response to sequence-specific binding to amplified DNA. This processing step results in a separation of the fluorophore and quencher groups, thereby leading to an increase in observable fluorescence.

Although the RPA reaction normally proceeds at 39 °C, we first tested whether it would proceed even at room temperature

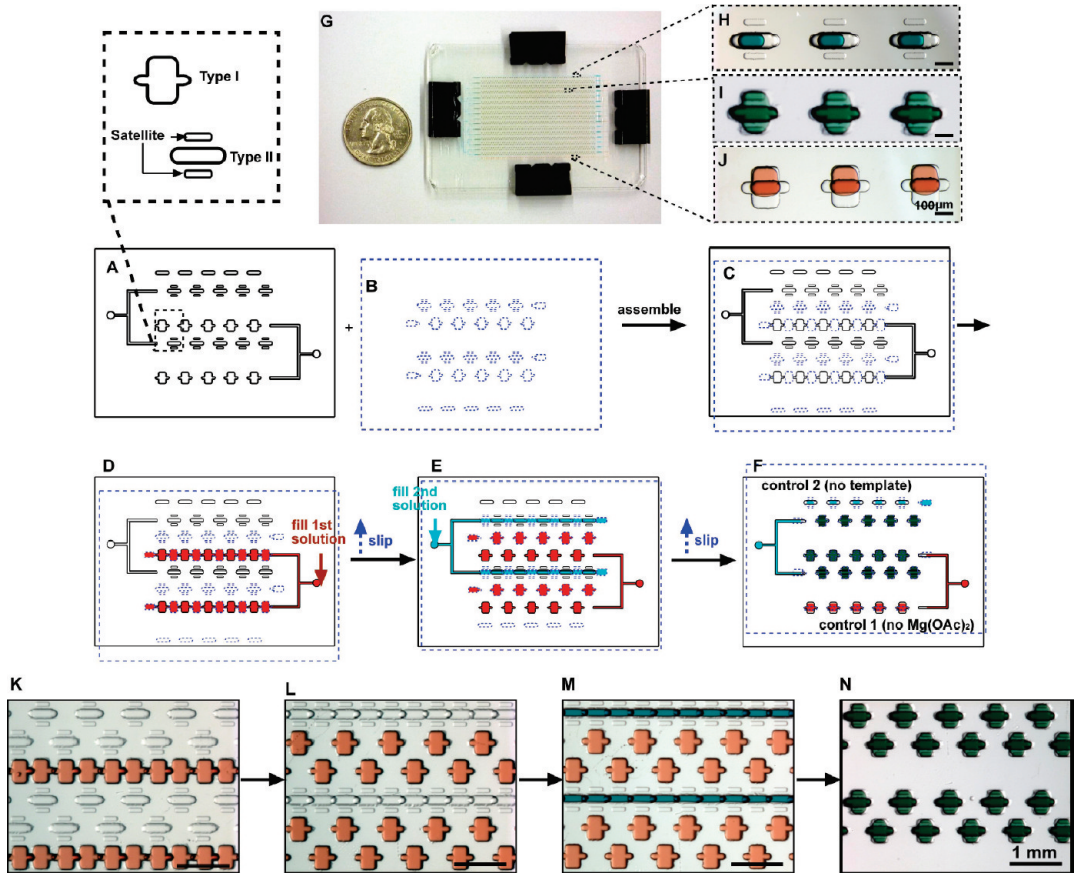


**Figure 2.** Schematic drawing of the two-step SlipChip for digital RPA. (A) Top plate of the SlipChip; a zoomed-in schematic drawing shows the geometry of type I, type II, and satellite wells. (B) Bottom plate of the SlipChip. (C) Assembly of top and bottom plates to establish the first continuous fluidic path of type I wells. (D) Loading of the first reagent, reaction mixture 1 (red). (E) Slipping breaks the first fluidic path and compartmentalizes the loaded reagent. At the same time, the second fluidic path is formed by connecting type II wells. The second reagent, reaction mixture 2 (light blue), is loaded through a second inlet. (F) A second slipping step compartmentalizes reaction mixture 2 into the type II wells and overlaps the type II wells with the type I wells. The two reagents are mixed within the reaction compartments. (G) Photograph shows the entire digital RPA SlipChip next to a U.S. quarter for size comparison. (H–J) Food dyes were loaded into the SlipChip to demonstrate loading and mixing. (H) Zoomed-in view of type II wells for control 2 (no template), loaded with blue food dye. (I) Zoomed-in view of reaction wells (overlapping type I and type II wells) containing mixed blue and orange food dye (green). (J) Zoomed-in view of type I wells for control 1 (no magnesium acetate), loaded with orange food dye. (K–N) Experiments with food dye demonstrate the procedures described in panels D–F.

(25 °C) upon mixing of the reagents in well plates, therefore potentially affecting the accuracy of the RPA results when performed in a digital format. The RPA solution was mixed with magnesium acetate and MRSA gDNA (final concentration of 5 pg/$\mu$L), then immediately placed in the plate reader (temperature controlled at 25 °C). The fluorescence intensity from wells containing gDNA template (Figure 1, green) started increasing within 20 min, which was significantly different from the fluorescent intensity of the control well without magnesium acetate (Figure 1, blue) and the control well without gDNA template (Figure 1, orange).

This result indicated that the RPA reaction amplified the target nucleic acid template in the presence of magnesium acetate at room temperature. Therefore, to achieve digital RPA without false-positive errors, the nucleic acid template must be compartmentalized first and then magnesium acetate should be added to each individual compartment. The noninitiating components of the RPA reaction mixture (RPA enzymes, buffer, primers, and probe) can be added to the solution containing nucleic acid template, to the solution of magnesium acetate, or to both.

To achieve this goal, we designed a SlipChip with two-step slipping that was able to load and compartmentalize two different reagents that could be combined by slipping (Figure 2). Each plate of the RPA SlipChip was designed to contain 800 wells of type I (6 nL) and 800 wells of type II (3 nL). Each type II well also had two satellite wells (0.2 nL) to address potential thermal expansion[51] during the temperature change from room temperature to 39 °C. The satellite wells provided additional space for thermal expansion of the aqueous reagent within the compartment formed by overlapping the type I and type II wells. A total of 1550 reaction compartments (9 nL each) were formed by overlapping the type I and type II wells contained in the facing plates (Figure 2, parts F, I, and N). The SlipChip also contained 50 wells for control 1 (type I wells, 6 nL, Figure 2, parts A, F, and J) and 50 wells for control 2 (type II wells, 3 nL, Figure 2, parts A, F, and H).

The digital RPA SlipChip was assembled by combining the top plate (Figure 2A) and bottom plate (Figure 2B) with a thin layer of tetradecane between as the lubricating fluid. The lubricating fluid prevented cross-contamination and evaporation of the aqueous sample during incubation. The first continuous


dx.doi.org/10.1021/ac200247e |*Anal. Chem.* 2011, 83, 3533–3540

fluidic path was formed by overlapping the type I wells in the two plates (Figure 2C). RPA reaction mixture 1, containing RPA primers and probe, MRSA gDNA, and rehydrated RPA enzyme mixture, but no magnesium acetate, was loaded by pipetting (Figure 2, parts D and K). This RPA SlipChip device was designed to be filled via dead-end filling; therefore, the speed of sample injection does not have to be controlled accurately as long as the applied pressure is lower than the leaking pressure.[52] The two plates were then slipped relative to one another to compartmentalize RPA reaction mixture 1, simultaneously stochastically confining the gDNA template in the type I wells and forming the second fluidic path by overlapping the type II wells (Figure 2, parts E and L). RPA reaction mixture 2, which contained no gDNA and contained magnesium acetate at 3-fold higher concentration than required for the bulk reaction (3×, so the final concentration of magnesium acetate after mixing would be 1×), RPA primers and probe, and rehydrated RPA enzyme, was also loaded into the chip by pipetting (Figure 2, parts E and M). Finally, the two plates were slipped relative to one another to overlap the type I wells with the type II wells in the facing plates, delivering the magnesium acetate in reaction mixture 2 to all 1550 of the type I wells simultaneously and initiating the reaction (Figure 2, parts F and N; Figure S1 in the Supporting Information shows loading of the digital RPA SlipChip with food dyes). The digital RPA SlipChip was then placed on a flat metal adapter and incubated at 39 °C for 1 h. Type I wells for control 1 contained only reaction mixture 1 (negative control, no magnesium acetate), and type II wells for control 2 contained only reaction mixture 2 (negative control, no nucleic acid template).

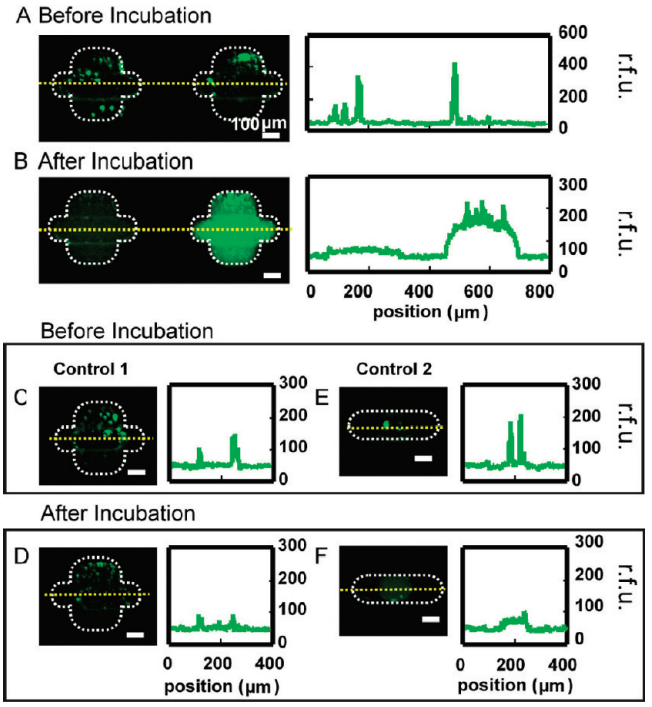


**Figure 3.** Fluorescence microphotographs and line scans of RPA on the SlipChip before and after incubation at 39 °C. (A and B) Negative (left) and positive (right) sample wells: (A) before incubation, the fluorescence intensity in both wells is the same; (B) after incubation, the integrated fluorescence intensity in the positive well (right) is significantly higher compared to that of the negative well (left). (C and D) Control well 1, containing no magnesium acetate, before (C) and after (D) incubation shows no significant increase in fluorescence intensity. (E and F) Control well 2, containing no gDNA template, before (E) and after (F) incubation also shows no significant increase in fluorescence intensity.

We first tested the digital RPA SlipChip with a sample containing a 1:$10^4$ dilution of 5 ng/μL of stock MRSA gDNA. The stock gDNA was purified from MRSA culture (see the Experimental Section in the Supporting Information), and the optical density of the purified nucleic acid product was measured spectrophotometrically. At this concentration, the average copy number of gDNA per well was expected to be less than 1, and single-copy RPA was achieved. The reaction solution of RPA was made from rehydrating the lyophilized reagent (see the Experimental Section in the Supporting Information) and was heterogeneous: microparticles of various sizes and shapes were still present even after sonication and vortexing the solution (Figure 3A, see the Experimental Section in the Supporting Information). A line scan of the fluorescence intensity of wells from the digital RPA SlipChip before and after incubation at 39 °C (Figure 3) shows that the fluorescence intensity of a positive well increased significantly compared to a negative well (Figure 3, parts A and B) and the control wells (Figure 3C−F) after incubation for 1 h. The number and the size of

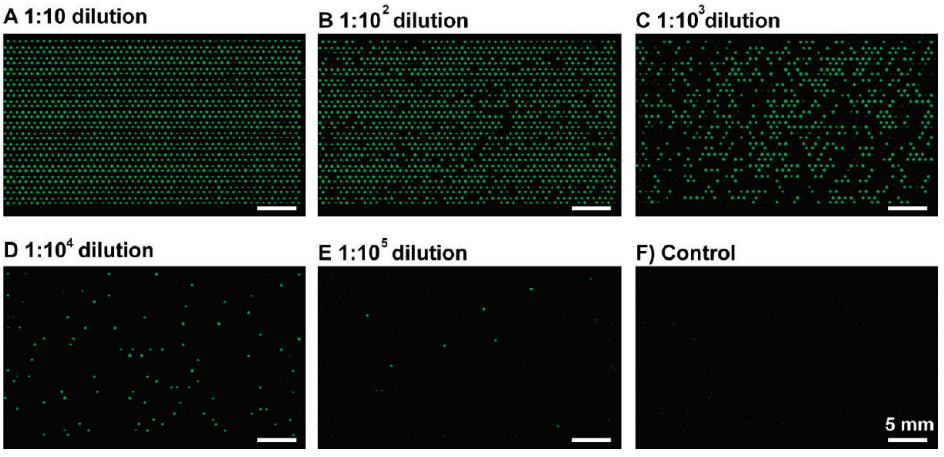


**Figure 4.** Digital RPA on the SlipChip with different concentration of MRSA gDNA. (A−E) Digital RPA on the SlipChip with a serial dilution of target DNA template ranging from 1:10 to 1:$10^5$ of a 5 ng/μL stock solution. (F) Control, no wells showed positive signal when no target DNA was loaded.

microparticles decreased after incubation, which was probably due to further dissolution of the microparticles during incubation at 39 °C. There was no significant increase of fluorescence intensity from control wells without magnesium acetate (representative control well 1, Figure 3, parts C and D) and without gDNA template (representative control well 2, Figure 3, parts E and F). Only the end point fluorescent intensity was monitored in this experiment. As demonstrated in previous work,[25] the amplification signal may be observed in less than 30 min. A real-time fluorescence detector would be useful to further investigate the uniformity of amplification and to optimize the total time required for incubation.

We characterized the performance of the digital RPA SlipChip using a serial dilution of the MRSA gDNA stock solution at 5 orders of magnitude, from 1:10 dilution to $1:10^5$ dilution. As the gDNA template was diluted, the fraction of positive wells on the RPA SlipChip decreased proportionally after incubation (Figure 4A–E and Figure 5). No evidence of contamination was observed as no false positives were observed in the control (no DNA template, Figure 4F). We repeated the experiments three times at each concentration of gDNA to test the robustness and reproducibility of the digital RPA on the SlipChip (Figure 5). The data from digital RPA on the SlipChip with serial-diluted gDNA template followed a Poisson distribution. A statistical analysis of the results from digital nucleic acid amplification on SlipChip was performed as previously described.[22] The initial stock concentration of MRSA gDNA was found to be approximately 10 million copies/mL by applying Most Probable Number (MPN) Theory to fit the results from the $1:10^3$, $1:10^4$, and $1:10^5$ dilutions. The expected results (Figure 5, black line) and 95% confidence interval (Figure 5, grey dashed lines) over the dilution range could then be calculated based on a Poisson distribution as described previously.[22]

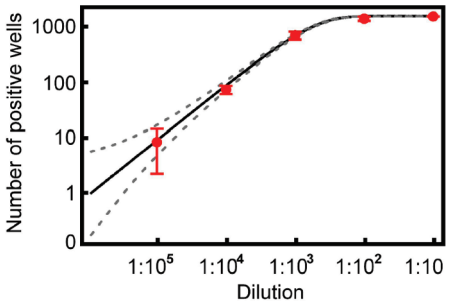


**Figure 5.** Quantified results of digital RPA on the SlipChip. Experimental average of the number of positive wells was plotted as a function of the dilution of the MRSA gDNA sample. Error bars represent standard deviation of the experiment ($n = 3$). The black solid line represents the Poisson distribution of the calculated stock concentration from fitting the data from the $1:10^5$, $1:10^4$, and $1:10^3$ dilutions of template. Gray dash lines represent the 95% confidence interval for the Poisson distribution.

The SlipChip design described above uses a two-step procedure for loading reagents: the two reagents can be loaded independently of one another, an attractive capability for general parallel processing of samples and reactions. Incubation or thermal cycling can be performed after confining the target molecules or the first reagent into individual reaction compartments, then additional reagents can be delivered (e.g., reagents for readout) into each compartment in parallel. This feature also facilitates quality control during development of new methods. Digital RPA requires parallel processing of reactions but does not specifically require two-step processing. Therefore, we have also tested a simplified device that does not have the capability to independently control reagents but instead allows compartmentalization and mixing of the two reaction mixtures in parallel by one-step slipping after simultaneous introduction of the reagents (Figure 6A–E). We have tested digital RPA with a $1:10^4$ dilution of MRSA gDNA template on this one-step SlipChip, and the result is consistent with the two-step SlipChip (Figure 6F, compare to Figure 7B, $n \geq 3$, $p > 0.2$)

We have shown that RPA can be initiated at room temperature (~25 °C) after magnesium acetate is added (Figure 1), and we have suggested that to achieve digital RPA, the reaction mixture containing target nucleic acid template must be separated into isolated reaction compartments before magnesium acetate is added. We tested this prediction more quantitatively on SlipChip: Instead of mixing reaction mixture 1 (without magnesium acetate) with reaction mixture 2 (with magnesium acetate)

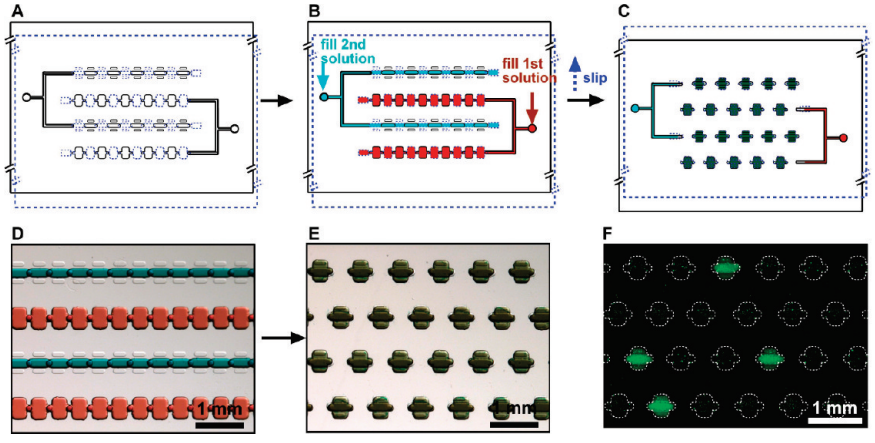


**Figure 6.** SlipChip for one-step digital RPA. (A–C) Schematic drawings of the SlipChip: (A) Assembly of top (solid) and bottom (dashed) plates to establish the continuous fluidic path for both type I wells and type II wells. (B) The first solution, reaction mixture 1 (red), and second solution, reaction mixture 2 (blue), are introduced simultaneously into the SlipChip. (C) Slipping breaks both fluidic paths and compartmentalizes the loaded reagent. At the same time, the type I wells are overlaid with type II wells to initiate the reaction. (D and E) Microphotographs showing food dyes loaded into the SlipChip to demonstrate loading and mixing. (F) Zoomed-in fluorescent image of a fraction of digital RPA on one-step SlipChip with a $1:10^4$ dilution of MRSA gDNA template after incubation at 39 °C.


dx.doi.org/10.1021/ac200247e |*Anal. Chem.* 2011, 83, 3533–3540

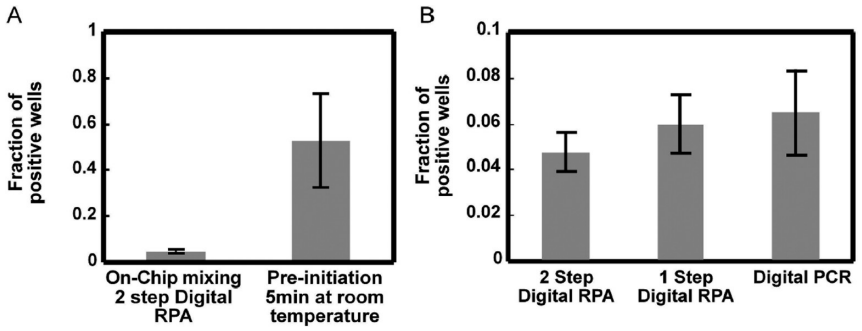


**Figure 7.** (A) Comparing on-chip mixing (no preinitiation) to preinitiation with magnesium acetate on the two-step digital RPA SlipChip. The sample with preinitiation with magnesium acetate prior to compartmentalization shows a higher fraction of positive wells, indicating that compartmentalization prior to the addition of magnesium acetate is crucial to achieve accurate digital RPA. (B) Comparing two-step digital RPA, one-step digital RPA, and digital PCR. Samples containing MRSA gDNA at the same dilution ($1{:}10^4$) were quantified using two-step digital RPA (as in Figure 4) (left, $n = 3$), one-step digital RPA (as in Figure 6) (middle, $n = 5$), and digital PCR (right, $n = 3$) on the RPA SlipChip. Error bars represent standard deviation.

on-chip, we mixed the reaction solution (containing a $1{:}10^4$ dilution of gDNA) with magnesium acetate to initiate the reaction off-chip, and incubated the solution at room temperature (~25 °C) for 1 min. We refer to this off-chip mixing and incubation as the "preinitiated" reaction solution. The preinitiated reaction solution was then injected into the two-step digital RPA SlipChip at room temperature through the type I wells and slipped to compartmentalize. The injection step took around 4 min. A second solution which contained magnesium acetate, RPA primers and probe, and rehydrated RPA enzyme was loaded into the type II wells as described above. Then, the type I and type II wells were overlaid by slipping the top plate relative to the bottom plate. The SlipChip was then incubated at 39 °C for 1 h. We compared these results to results obtained without preinitiating the solution with magnesium acetate off-chip (from experiments shown in Figures 4 and 5). The fraction of positive wells from the preinitiated sample was significantly higher than in the sample without preinitiation (Figure 7A, $n = 3$, $p < 0.01$). We attribute the large standard deviation in the measurement of the preinitiated sample to the variation in loading time that would change the extent of reaction prior to compartmentalization; reaction taking place during loading is also consistent with the "streaky" distribution of the positive wells in these experiments (see Figure S2 in the Supporting Information). These results confirm that compartmentalization followed by chemical initiation of the RPA reaction is essential to obtain quantitative results using digital RPA.

To further validate the performance of digital RPA on the SlipChip, we compared experiments of digital RPA to experiments of digital PCR using the same concentration of MRSA gDNA on the same SlipChip ($1{:}10^4$ dilution, see the Experimental Section and Figure S3 in the Supporting Information). The same *mecA* gene in MRSA gDNA was targeted for quantification in both methods. The average results from two-step digital RPA and one-step digital RPA were not significantly different ($p > 0.2$, $n \geq 3$) than from digital PCR (Figure 7B). Because RPA does not benefit from the high-temperature step employed in PCR, one potential concern regarding the use of digital RPA is sensitivity to secondary structures of nucleic acids or to contamination with nucleic acid binding proteins; this could lead to lower "counts" of nucleic acids. To address this concern, RPA was designed to operate in the presence of comparatively large amounts of gp32, the single-strand binding protein from T4-like bacteriophages. Gp32 has been reported to bind ssDNA and "melt" secondary DNA structures.[53] It has also been used as a common enhancer of various molecular biology techniques, including PCR and reverse transcription.[54] Further work will be clearly needed to evaluate relative performance of digital PCR and digital RPA over a wide range of DNA targets produced by different sample preparation protocols.

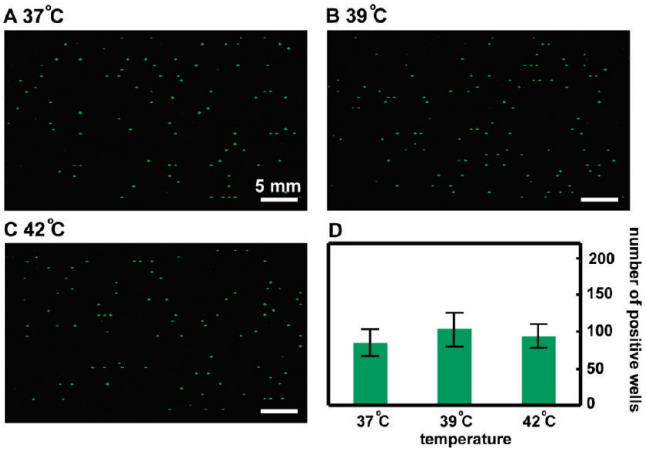


**Figure 8.** RPA two-step SlipChip for amplification of MRSA gDNA with incubation at different temperatures. (A–C) Representative fluorescent images of RPA for MRSA gDNA with dilution of $1{:}10^4$ at 37 (A), 39 (B), and 42 °C (C). (D) Histogram showing number of positive wells from RPA on the SlipChip at different incubation temperatures. Error bars represent standard deviation of the experiment ($p > 0.2$, $n \geq 4$).

The digital RPA SlipChip depends on the end point fluorescence reading of either "0" or "1", unlike real-time PCR and real-time RPA[25] which monitor the change of fluorescence intensity over time. Since the enzyme activity depends on the working temperature, the temperature dramatically affects the amplification speed in real-time RPA. Therefore, real-time amplification methods require accurate control of temperature and careful calibration for quantitative analysis. This may make real-time RPA less applicable in point-of-care diagnostics in resource-limited settings. Because the digital RPA SlipChip detects only the end point readout instead of real-time changes of fluorescent intensity, the digital RPA SlipChip was expected to be more tolerant to temperature fluctuations than real-time methods. Indeed, we found that amplification of MRSA gDNA at 37, 39, and 42 °C was not significantly different (Figure 8, $p > 0.2$, $n \geq 4$).

We also found that increasing the temperature decreases the required incubation time and quantitative results can be achieved in as short as 30 min with incubation under 42 °C.

## CONCLUSION

Here we have demonstrated that parallel initiation of pre-compartmentalized reactions on the SlipChip lends itself to isothermal nucleic acid quantification by using recombinase polymerase amplification (RPA) at 39 °C in a digital format. The RPA reaction will start even at room temperature once the magnesium acetate is added into the reaction mixture, increasing the number of false positives in digital RPA if the reaction mixture is compartmentalized after off-chip mixing of all reagents with the nucleic acid template. The digital RPA SlipChip addressed this issue straightforwardly by first separating the reaction mixture containing nucleic acid template into individual compartments, in the absence of magnesium acetate and then delivering magnesium acetate to all compartments simultaneously by slipping. A one-step SlipChip was also demonstrated and validated using digital RPA, and the result was consistent with the results obtained on the two-step SlipChip. The digital RPA SlipChip was also demonstrated to be robust in the presence of small perturbations of incubation temperature from 37 to 42 °C. The digital RPA SlipChip was designed to contain 1550 reaction compartments of 9 nL each, with two additional sets of wells for controls (50 wells for each control), giving a potential for detection limit of 300 copies/mL and dynamic range of 1400−1 000 000 copies/mL with 3-fold resolution, calculated using the method described previously.[22] The RPA reaction was robust and free of cross-contamination on the SlipChip. However, microparticles were present in the reaction mixture even after vortexing and sonication, and additional optimization and investigation of the RPA reaction mixture may be required to determine how the number and size of these microparticles may affect the amplification reaction. A real-time imaging system would validate the uniformity of the amplification rate in each positive well. No false-positive results were observed in the experiments, but the specificity of the device and strategy for multiplex detection remain to be tested. Incorporation of a reverse-transcription step with RPA will expand the applicability of the digital RPA SlipChip for quantitative analysis of viral loads in resource-limited areas in developing countries. With these developments, this methodology would provide a platform for quantification of nucleic acids under resource-limited settings and in the clinic, where digital PCR and real-time PCR may not be available due to limited infrastructure.[1−11] In situations where the infrastructure for PCR is available, the digital PCR SlipChip[22] may be preferred because all the reagents and template can be loaded as one solution. SlipChip fabricated from plastic materials[52] could further lower the cost and make the device disposable to avoid potential contamination from reusing the devices. More broadly, this methodology should find a number of applications that require or rely on initiation of thousands of chemical reactions in parallel using simple, solvent-resistant glass or plastic[52] devices.

## ASSOCIATED CONTENT

**Supporting Information.** Chemicals and materials, detailed experimental procedures, and additional figures. This material is available free of charge via the Internet at http://pubs.acs.org.

## AUTHOR INFORMATION

**Corresponding Author**
*E-mail: r-ismagilov@uchicago.edu.

## ACKNOWLEDGMENT

This work was supported by the NIH Director's Pioneer Award program, part of the NIH Roadmap for Medical Research (1 DP1 OD003584), NIH Grant No. 1R01 EB012946 administered by the National Institute of Biomedical Imaging and Bioengineering, and by the W. M. Keck Foundation. Part of this work was performed at the Materials Research Science and Engineering Centers microfluidics facility (funded by the National Science Foundation). We thank Kevin P. Nichols for assisting with fabrication of the SlipChip. We thank Heidi Park for contributions to writing and editing this manuscript.

## REFERENCES

(1) Livak, K. J.; Schmittgen, T. D. *Methods* **2001**, *25*, 402–408.
(2) Vet, J. A. M.; Majithia, A. R.; Marras, S. A. E.; Tyagi, S.; Dube, S.; Poiesz, B. J.; Kramer, F. R. *Proc. Natl. Acad. Sci. U.S.A.* **1999**, *96*, 6394–6399.
(3) Mackay, I. M.; Arden, K. E.; Nitsche, A. *Nucleic Acids Res.* **2002**, *30*, 1292–1305.
(4) Jarvius, J.; Melin, J.; Goransson, J.; Stenberg, J.; Fredriksson, S.; Gonzalez-Rey, C.; Bertilsson, S.; Nilsson, M. *Nat. Methods* **2006**, *3*, 725–727.
(5) Vogelstein, B.; Kinzler, K. W. *Proc. Natl. Acad. Sci. U.S.A.* **1999**, *96*, 9236–9241.
(6) Nacht, M.; Dracheva, T.; Gao, Y. H.; Fujii, T.; Chen, Y. D.; Player, A.; Akmaev, V.; Cook, B.; Dufault, M.; Zhang, M.; Zhang, W.; Guo, M. Z.; Curran, J.; Han, S.; Sidransky, D.; Buetow, K.; Madden, S. L.; Jen, J. *Proc. Natl. Acad. Sci. U.S.A.* **2001**, *98*, 15203–15208.
(7) Cheng, B.; Landay, A.; Miller, V. *Curr. Opin. HIV AIDS* **2008**, *3*, 495–503.
(8) Preiser, W.; Drexler, J. F.; Drosten, C. *PLoS Med.* **2006**, *3*, e538; author reply e550.
(9) UNAIDS/WHO. *2008 Report on the Global AIDS Epidemic*; UNAIDS/WHO: Geneva, Switzerland, 2008.
(10) Fan, H. C.; Quake, S. R. *Anal. Chem.* **2007**, *79*, 7576–7579.
(11) Lo, Y. M. D.; Lun, F. M. F.; Chan, K. C. A.; Tsui, N. B. Y.; Chong, K. C.; Lau, T. K.; Leung, T. Y.; Zee, B. C. Y.; Cantor, C. R.; Chiu, R. W. K. *Proc. Natl. Acad. Sci. U.S.A.* **2007**, *104*, 13116–13121.
(12) Heid, C. A.; Stevens, J.; Livak, K. J.; Williams, P. M. *Genome Res.* **1996**, *6*, 986–994.
(13) Gibson, U. E. M.; Heid, C. A.; Williams, P. M. *Genome Res.* **1996**, *6*, 995–1001.
(14) Kalinina, O.; Lebedeva, I.; Brown, J.; Silver, J. *Nucleic Acids Res.* **1997**, *25*, 1999–2004.
(15) Sykes, P. J.; Neoh, S. H.; Brisco, M. J.; Hughes, E.; Condon, J.; Morley, A. A. *BioTechniques* **1992**, *13*, 444–449.
(16) Beer, N. R.; Wheeler, E. K.; Lee-Houghton, L.; Watkins, N.; Nasarabadi, S.; Hebert, N.; Leung, P.; Arnold, D. W.; Bailey, C. G.; Colston, B. W. *Anal. Chem.* **2008**, *80*, 1854–1858.
(17) Kiss, M. M.; Ortoleva-Donnelly, L.; Beer, N. R.; Warner, J.; Bailey, C. G.; Colston, B. W.; Rothberg, J. M.; Link, D. R.; Leamon, J. H. *Anal. Chem.* **2008**, *80*, 8975–8981.
(18) Leng, X. F.; Zhang, W. H.; Wang, C. M.; Cui, L. A.; Yang, C. J. *Lab Chip* **2010**, *10*, 2841–2843.
(19) Ottesen, E. A.; Hong, J. W.; Quake, S. R.; Leadbetter, J. R. *Science* **2006**, *314*, 1464–1467.

(20) Sundberg, S. O.; Wittwer, C. T.; Gao, C.; Gale, B. K. *Anal. Chem.* **2010**, *82*, 1546–1550.
(21) Applied Biosystems, Life Technologies. TaqMan OpenArray Digital PCR Plates. https://products.appliedbiosystems.com/ab/en/US/adirect/ab?cmd=catNavigate2&catID=607965 (accessed December 17, 2010).
(22) Shen, F.; Du, W. B.; Kreutz, J. E.; Fok, A.; Ismagilov, R. F. *Lab Chip* **2010**, *10*, 2666–2672.
(23) Notomi, T.; Okayama, H.; Masubuchi, H.; Yonekawa, T.; Watanabe, K.; Amino, N.; Hase, T. *Nucleic Acids Res.* 2000, *28*, e63.
(24) Compton, J. *Nature* **1991**, *350*, 91–92.
(25) Piepenburg, O.; Williams, C. H.; Stemple, D. L.; Armes, N. A. *PLoS Biol.* **2006**, *4*, 1115–1121.
(26) Lizardi, P. M.; Huang, X. H.; Zhu, Z. R.; Bray-Ward, P.; Thomas, D. C.; Ward, D. C. *Nat. Genet.* **1998**, *19*, 225–232.
(27) Vincent, M.; Xu, Y.; Kong, H. M. *EMBO Rep.* **2004**, *5*, 795–800.
(28) Hill, C.; Bott, M.; Clark, K.; Jonas, V. *Clin. Chem.* **1995**, *41*, S107–S107.
(29) Chelliserrykattil, J.; Nelson, N. C.; Lyakhov, D.; Carlson, J.; Phelps, S. S.; Kaminsky, M. B.; Gordon, P.; Hashima, S.; Ngo, T.; Blazie, S.; Brentano, S. *J. Mol. Diagn.* **2009**, *11*, 680–680.
(30) Dean, F. B.; Hosono, S.; Fang, L. H.; Wu, X. H.; Faruqi, A. F.; Bray-Ward, P.; Sun, Z. Y.; Zong, Q. L.; Du, Y. F.; Du, J.; Driscoll, M.; Song, W. M.; Kingsmore, S. F.; Egholm, M.; Lasken, R. S. *Proc. Natl. Acad. Sci. U.S.A.* **2002**, *99*, 5261–5266.
(31) Walker, G. T.; Fraiser, M. S.; Schram, J. L.; Little, M. C.; Nadeau, J. G.; Malinowski, D. P. *Nucleic Acids Res.* **1992**, *20*, 1691–1696.
(32) Hellyer, T. J.; Nadeau, J. G. *Expert Rev. Mol. Diagn.* **2004**, *4*, 251–261.
(33) Mazutis, L.; Araghi, A. F.; Miller, O. J.; Baret, J. C.; Frenz, L.; Janoshazi, A.; Taly, V.; Miller, B. J.; Hutchison, J. B.; Link, D.; Griffiths, A. D.; Ryckelynck, M. *Anal. Chem.* **2009**, *81*, 4813–4821.
(34) Blainey, P. C.; Quake, S. R. *Nucleic Acids Res.* **2011**, *39*, e19.
(35) Fang, X. E.; Liu, Y. Y.; Kong, J. L.; Jiang, X. Y. *Anal. Chem.* **2010**, *82*, 3002–3006.
(36) Dimov, I. K.; Garcia-Cordero, J. L.; O'Grady, J.; Poulsen, C. R.; Viguier, C.; Kent, L.; Daly, P.; Lincoln, B.; Maher, M.; O'Kennedy, R.; Smith, T. J.; Ricco, A. J.; Lee, L. P. *Lab Chip* **2008**, *8*, 2071–2078.
(37) Esch, M. B.; Locascio, L. E.; Tarlov, M. J.; Durst, R. A. *Anal. Chem.* **2001**, *73*, 2952–2958.
(38) Lutz, S.; Weber, P.; Focke, M.; Faltin, B.; Hoffmann, J.; Muller, C.; Mark, D.; Roth, G.; Munday, P.; Armes, N.; Piepenburg, O.; Zengerle, R.; von Stetten, F. *Lab Chip* **2010**, *10*, 887–893.
(39) Birch, D. E.; Laird, W. J.; Zoccoli, A. Nucleic acid amplification using a reversibly inactivated thermostable enzyme. United States Patent US5773258, June 30, 1998.
(40) Liu, J.; Hansen, C.; Quake, S. R. *Anal. Chem.* **2003**, *75*, 4718–4723.
(41) Thorsen, T.; Maerkl, S. J.; Quake, S. R. *Science* **2002**, *298*, 580–584.
(42) Song, H.; Tice, J. D.; Ismagilov, R. F. *Angew. Chem., Int. Ed.* **2003**, *42*, 768–772.
(43) Tewhey, R.; Warner, J. B.; Nakano, M.; Libby, B.; Medkova, M.; David, P. H.; Kotsopoulos, S. K.; Samuels, M. L.; Hutchison, J. B.; Larson, J. W.; Topol, E. J.; Weiner, M. P.; Harismendy, O.; Olson, J.; Link, D. R.; Frazer, K. A. *Nat. Biotechnol.* **2009**, *27*, 1025–1031.
(44) Li, L.; Boedicker, J. Q.; Ismagilov, R. F. *Anal. Chem.* **2007**, *79*, 2756–2761.
(45) Zheng, B.; Ismagilov, R. F. *Angew. Chem., Int. Ed.* **2005**, *44*, 2520–2523.
(46) Brouzes, E.; Medkova, M.; Savenelli, N.; Marran, D.; Twardowski, M.; Hutchison, J. B.; Rothberg, J. M.; Link, D. R.; Perrimon, N.; Samuels, M. L. *Proc. Natl. Acad. Sci. U.S.A.* **2009**, *106*, 14195–14200.
(47) Du, W. B.; Li, L.; Nichols, K. P.; Ismagilov, R. F. *Lab Chip* **2009**, *9*, 2286–2292.
(48) Liu, W. S.; Chen, D. L.; Du, W. B.; Nichols, K. P.; Ismagilov, R. F. *Anal. Chem.* **2010**, *82*, 3276–3282.
(49) Li, L.; Du, W.; Ismagilov, R. F. *J. Am. Chem. Soc.* **2009**, *132*, 112–119.
(50) Li, L.; Ismagilov, R. F. *Annu. Rev. Biophys.* **2010**, *39*, 139–158.
(51) Shen, F.; Du, W. B.; Davydova, E. K.; Karymov, M. A.; Pandey, J.; Ismagilov, R. F. *Anal. Chem.* **2010**, *82*, 4606–4612.
(52) Li, L. A.; Karymov, M. A.; Nichols, K. P.; Ismagilov, R. F. *Langmuir* **2010**, *26*, 12465–12471.
(53) Shamoo, Y.; Friedman, A. M.; Parsons, M. R.; Konigsberg, W. H.; Steitz, T. A. *Nature* **1995**, *376*, 362–366.
(54) Piche, C.; Schernthaner, J. P. *J. Biomol. Tech.* **2005**, *16*, 239–247.